

CO₂ Fixation by Alkylzinc Amides: A Quantum Chemical Study Motivated by Recent Experimental Results

Hans-Jörg Himmel*^[a]

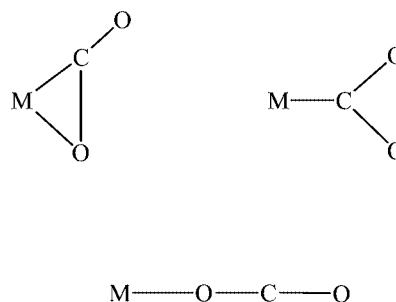
Keywords: CO₂ fixation / Zinc / Reaction mechanisms / Quantum chemical calculations

Herein the insertion of CO₂ into the Zn–N bond of alkylzinc amides of the general formula RZnNR'₂ (R = H, CH₃, CF₃, R' = CH₃, *i*Pr, H, F, C₆H₅) is discussed on the basis of quantum chemical calculations. Several possible reaction pathways were considered, starting from monomeric as well as dimeric alkylzinc amides. Special consideration is given to the influence of the electronic properties of the amido group on the reaction energy. The mechanisms were studied in detail starting with the model compounds HZnNH₂ and H₃CZnN(CH₃)₂ as well as the dimer [HZnNH₂]₂. The reaction of monomeric compounds with CO₂ first leads to an intermediate featuring a Zn–N–C–O four-membered ring. This first step requires an activation energy ΔG of ca. 60 kJ·mol^{–1} and turns out to be the rate-determining step. In the second step, which requires a much smaller activation energy, the

carbamate product is formed. Reactions of dimeric alkylzinc amides are subject to a significantly higher activation barrier (with a ΔG value of 103 kJ·mol^{–1}), with a four-membered ring as the transition-state structure. The activation energy is slightly higher than the energy required for decomposition of the dimer into two monomers, and therefore it is plausible that the alkylzinc amides react as monomers with CO₂. The calculations for the dimer reaction again gave evidence for the formation of an intermediate exhibiting in this case a six-membered ring. The barrier to formation of the carbamate from this intermediate is very small. The results of this work contribute to the knowledge of CO₂ fixation by alkylzinc amides and might shed some light on enzymatic reactivity. (© Wiley-VCH Verlag GmbH & Co. KGaA, 69451 Weinheim, Germany, 2007)

Introduction

The reduction of CO₂ emission, a gas that besides others is responsible for global warming, is continuing to be an extremely important issue, especially since no real alternatives to fossil fuels^[1] have yet been discovered. Therefore, there is a great demand for methods to either reduce CO₂ production or for suitable materials that help to reduce the release of the produced CO₂ into the air (and ideally turn CO₂ into something useful at the same time). There are now numerous examples of transition-metal complexes that can bind CO₂.^[2] In the case of mononuclear complexes three coordination modes can be realized (see Scheme 1). The first authenticated example for the η^1 -OCO binding mode was discovered only very recently,^[3] although it seems to play an important role in enzymes. In this example a linear CO₂ unit is bound to a trivalent uranium atom in the center of a sterically crowded complex. The unusual coordination mode most likely results from the restricted space that the ligand shell offers to the incoming CO₂.

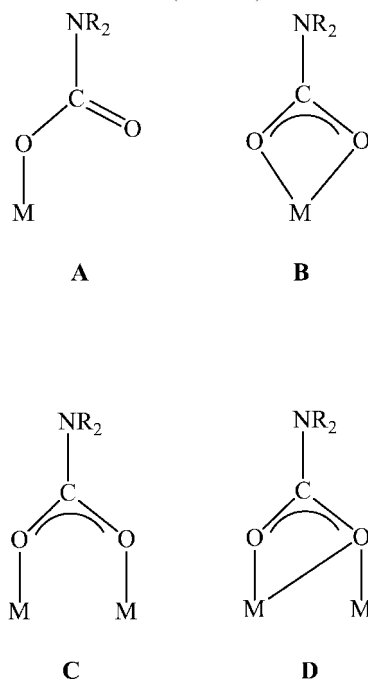


Scheme 1.

Several main-group element compounds are also known to react with CO₂. Very recently it was claimed that the reaction of Mg[N(SiMe₃)₂]₂ with AlR₃ (R = Me or Et) and CO₂ in THF affords aluminium–magnesium complexes with linearly bridging CO₂ units, viz. [{R₂Al(μ-NSiMe₃)(μ-OSiMe₃)Mg(thf)₂(μ-O₂C)}₃].^[4] However, this result was questioned by a later analysis,^[5] according to which the compound exhibits bridging NCO[–] ligands instead of the isoelectronic neutral CO₂ ligands. Zn compounds, especially pyrazolylborate zinc hydroxides,^[6] dinuclear complexes that should mimic the reactive center of enzymes,^[7] and zinc amides (see below), were also the focus of recent research, particularly because of their biological relevance.

[a] Anorganisch-Chemisches Institut, Ruprecht-Karls-Universität Heidelberg
Im Neuenheimer Feld 270, 69120 Heidelberg, Germany
Fax: +49-6221-54-5707
E-mail: hans-jorg.himmel@aci.uni-heidelberg.de

Several amides of main group elements (such as Li or Mg) have been shown to react with CO₂ to give carbamate molecules. Generally four bonding modes can be realized (see Scheme 2).^[8] The enzyme rubisco (ribulose-1,5-bisphosphate-carboxylase/oxygenase) features a Mg²⁺ ion in the center to which a monodentate carbamate ligand is bound (thus realizing bonding mode A).^[9,10] Bonding mode C is realized, for example, in the enzymes urease and phosphotriesterase in which a carbamate ligand (formed from a lysine) bridges two nickel (urease) or zinc (phosphotriesterase) ions.^[10,11] The first example for bonding mode B was found only very recently in the unsymmetrical dinuclear compound [Mg₂(O₂CNCy₂)₄(HMPA)], where Cy = cyclohexyl and HMPA = hexamethylphosphoramide.^[12] There are several synthetic routes to carbamates, one of which is a direct reaction of amides with CO₂.^[2] It was shown that chiral carbamates can be synthesized from the reaction between chiral lithium amides and CO₂.^[13] The mechanism for these reactions was recently analyzed on the basis of quantum chemical (B3LYP) calculations.^[14]



Scheme 2.

The reactions between alkylzinc amides of the formula RZnNEt₂ (R = Me, Et) and CO₂ were reported to first give the tetramer [R₂Zn₄O₂C(NEt₂)₆]^[15] which reacts with an excess of ZnMe₂ to give the compound [Zn₄Me₄(O₂CNEt₂)₄] featuring an approximately tetrahedral arrangement of the four Zn atoms.^[16] Very recently it was shown that CO₂ inserts into the metal–nitrogen bond of H₃CZnNR₂ (R = *i*Pr, *i*Bu or piperidiny) to give tetrameric cage compounds of the formula [H₃CZnO₂CNR₂]₄,^[17] which seem to contradict previously obtained results. Interestingly, addition of pyridine achieves a breakage of the tetramer into two dimeric units. In light of all these findings a theoretical analysis of the reaction pathways is highly desirable.

Results and Discussion

The discussion is divided into two sections. In the first one it is assumed that the alkylzinc amide reacts as a monomer with CO₂, although of course the majority of alkylzinc amides are generally expected to be dimeric or even trimeric. However, monomeric alkylzinc amides containing sterically demanding alkyl groups are known, e.g. (Me₃Si)₃CZnN(H)Si(*i*Pr₃).^[18] It is assumed that the reaction first leads to a monomeric zinc carbamate, which oligomerizes afterwards. In the second section CO₂ fixation by dimeric alkylzinc amides is discussed.

1. Reactions Starting from Monomeric Alkylzinc Amides

Although monomeric alkylzinc amides can only be isolated in the case of sterically demanding alkyl groups, they could in other cases exist in solution (in small quantities) in equilibrium with the dimeric form.^[19] The general consensus in the case of mononuclear transition-metal complexes is that electrophilic attack at the amide nitrogen by the carbon atom of CO₂ initiates reaction. However, the role of the metal has not yet been accessed in sufficient depth. In the case of *fac*-(CO)₃(dppe)MnOR derivatives featuring an alkoxide or aryloxy (OR) group in place of an amide a four-membered transition state has been postulated.^[20] In this transition state, the C atom of the CO₂ group interacts with the O atom of the OR group, and one of the O atoms of CO₂ interacts with the metal center. This suggestion might imply that the metal–oxygen interaction is already established at an early stage of the reaction. One of the objectives of the following discussion is therefore to analyze the role of the metal–oxygen bond during the reactions of alkylzinc amides with CO₂. However, other questions concerning the mechanism arise. In the case of insertion of CO₂ into the metal–nitrogen bond of the transition-metal complex (Ph)(PCy₃)₂PtNH₂^[21] it was claimed, on the basis of spectroscopic (IR, NMR) evidence, that in benzene a nitrogen-bonded carbamate is first formed. This species was reported to rearrange readily when dissolved in dichloromethane to the more stable oxygen-bonded carbamate. Thus the calculations in this paper also have to answer the question whether or not the nitrogen-bonded carbamate represents an intermediate in the course of the reaction with alkylzinc amides.

The analysis starts with the simplest possible model compound, cf. HZnNH₂. Two different initial orientations of the CO₂ molecule were considered. In the first one the O–C–O axis is oriented perpendicular to the H–Zn–N plane (“vertical” approach). The CO₂ axis at the start of the reaction has roughly the same relative orientation as in the product. The symmetry is constrained to C_{2v} throughout the approach of the CO₂ toward the alkylzinc amide. Figure 1 displays the energy as calculated using BP/TZVPP relative to that of the two separated reactants (HZnNH₂ and CO₂) versus the Zn–N–C angle. The CO₂ molecule already occurs at large values of the reaction coordinate, slightly attracted by the lone pair at the N atom. For a Zn–N–C

angle of 112.2°, a minimum is reached at a relative energy of not more than $-8 \text{ kJ}\cdot\text{mol}^{-1}$ (according to BP/TZVPP). The N...C separation at this point amounts to 295.7 pm. The C–O distances (117.2 pm) are almost identical to those in free CO₂ (117.1 pm according to our BP/TZVPP calculations, exp. value: 116.32 pm). The Zn–N distance measures 183.7 pm and is also only very slightly elongated relative to the distance in free HZnNH₂ (183.1 pm). If the molecule is restricted to C_{2v} symmetry the energy again increases for smaller values of the reaction coordinate, and no binding interaction between the O atoms and the Zn atom is established. The interaction energy between the amido group and the CO₂ under these conditions is thus only $-8 \text{ kJ}\cdot\text{mol}^{-1}$, a value too weak to bring about reaction. This is a first result underlining the importance of an early formation of a metal–oxygen interaction for any further reaction to occur.

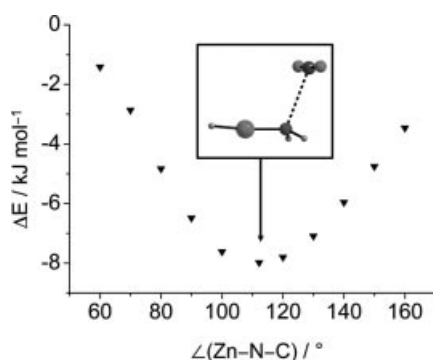


Figure 1. Energy versus the Zn–N–C angle and relative to the separated reactants for the “vertical” approach of the CO₂ molecule toward monomeric HZnNH₂ as calculated with BP/TZVPP. The inset shows the structure of the minimum.

The second possibility is that at an early stage of the reaction the three atoms of the CO₂ molecule are located roughly in the same plane as the H, Zn, and N atoms of the alkylzinc amide (“parallel” approach). Of course, in this case the symmetry has to change somewhere along the reaction coordinate and therefore all calculations were carried out in C₁ symmetry.^[22] Figure 2 shows the relative energy calculated versus the N–C distance. Again a shallow minimum (ΔE of ca. $8 \text{ kJ}\cdot\text{mol}^{-1}$ without ZPE corrections) occurs at large N–C distances (centered at 280 pm). However, after the system has passed a first transition state (with ΔE being +7 without and +18 kJ·mol⁻¹ with ZPE corrections, and ΔG being +59 kJ·mol⁻¹) it reaches a local minimum that is bound with respect to the reactants by $-19 \text{ kJ}\cdot\text{mol}^{-1}$ without and $-8 \text{ kJ}\cdot\text{mol}^{-1}$ with ZPE corrections. At +33 kJ·mol⁻¹ the ΔG value is still positive at this point. This local minimum features a four-membered [ZnNCO] ring and is characterized by the following bond lengths (in pm, for BP/TZVPP): 155.1 (N–C), 102.4 (N–H), 120.8/129.6 (C–O), 151.7 (Zn–H), 196.1 (Zn–O), and 252.7 (Zn–N). The C–O bond as part of the four-membered ring is significantly elongated (129.6 pm) to a value that falls in between the typical regions for CO single (ca. 142 pm) and double bonds. At 132.0° the O–C–O bond angle is already quite

small. A significant Zn–O interaction is already established and, together with a larger C–N interaction, is responsible for the decrease in energy. The Zn–N distance at this point is substantially elongated with respect to that in free HZnNH₂ (183.1 pm). However, the formation of new bonds can more than compensate the decrease of the Zn–N bond strength. For N–C distances shorter than 155.1 pm, the relative energy first slightly rises until, at ca. 145 pm, a second transition state is reached. The energy at this transition state is not more than $6 \text{ kJ}\cdot\text{mol}^{-1}$ higher than that of the preceding local minimum. Relative to the reactants the energy at this point amounts to -13 without and $-1 \text{ kJ}\cdot\text{mol}^{-1}$ with ZPE corrections, and ΔG is +40 kJ·mol⁻¹. Finally, at an N–C distance of 135.5 pm, the carbamate product is reached, which adopts the structure type **B** (see Scheme 2). The energy of the carbamate is by -79 or $-67 \text{ kJ}\cdot\text{mol}^{-1}$ (without or with ZPE corrections, respectively) lower than that of the two separated reactants. ΔG for the complete reaction is $-26 \text{ kJ}\cdot\text{mol}^{-1}$. The Zn–H, Zn–O, C–O, and N–H distances were calculated to be 151.8, 204.6, 128.9, and 101.0 pm, respectively. The Zn...N separation now amounts to 236.2 pm and the O–C–O angle measures 119.9°. This compares to an O–C–O angle of 119.63(16)° in the compound [Mg₂(O₂CNCy₂)₄(HMPA)] (see Introduction), the only known example of mode **B** in Mg chemistry.^[12]

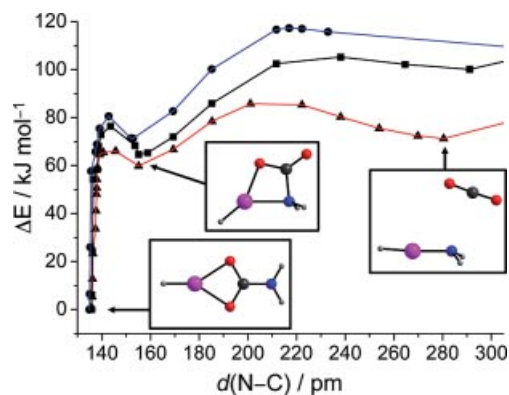


Figure 2. Energy relative to the carbamate product versus the N–C distance as calculated for the reaction of CO₂ with HZnNH₂ (BP/TZVPP calculation, red line), H₃CZnN(CH₃)₂ (BP/TZVPP calculation, black line) and H₃CZnN(CH₃)₂ (B3LYP/TZVPP calculation, blue line).

There is no evidence for the formation of a nitrogen-bonded carbamate as an intermediate in the course of the reaction. Nevertheless, we have calculated the geometry and energy of such a species. Its energy turned out to be $12 \text{ kJ}\cdot\text{mol}^{-1}$ according to BP/SVP and $7 \text{ kJ}\cdot\text{mol}^{-1}$ according to BP/TZVPP higher than that of the intermediate four-membered ring that is formed during the reaction. This value is higher than the barrier to carbamate formation (second TS, see Table 1) and it is not likely that interaction with the solvent (toluene) leads to a significant stabilization. Therefore any engagement of the nitrogen-bonded carbamate in the reaction can be ruled out. Figure 3 summarizes the reaction pathway.^[23]

Table 1. Energy, ΔE , zero-point energy corrected energy, ΔE_{ZPE} , and ΔG (at 298 K, 1 bar), all in $\text{kJ}\cdot\text{mol}^{-1}$, relative to the reactants for the reaction between HZnNH_2 or $\text{H}_3\text{CZnN}(\text{CH}_3)_2$ and CO_2 as calculated with BP/TZVPP and B3LYP/TZVPP.

	HZnNH_2	$\text{H}_3\text{CZnN}(\text{CH}_3)_2$	
	BP/TZVPP	BP/TZVPP	B3LYP/TZVPP
	$\Delta E, \Delta E_{\text{ZPE}}, \Delta G$	$\Delta E, \Delta E_{\text{ZPE}}, \Delta G$	$\Delta E, \Delta E_{\text{ZPE}}, \Delta G$
First TS ^[a]	+7, +18, +59	+1, +12, +56	+8, +19, +63
Intermediate	-19, -8, +33	-40, -29, +15	-38, -27, +17
Second TS ^[a]	-13, -1, +40	-28, -16, +29	-29, -17, +28
Product	-79, -67, -26	-105, -93, -50	-109, -97, -54

[a] TS: transition state.

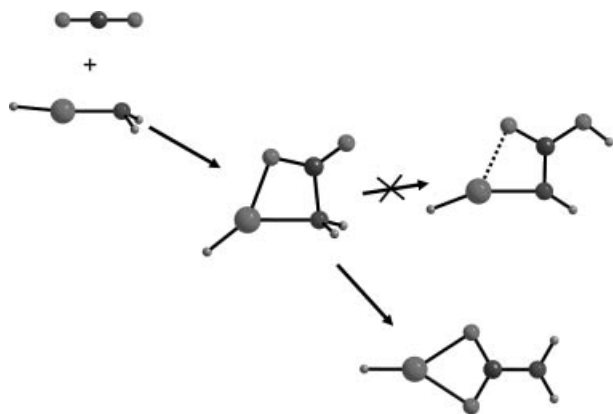


Figure 3. Pathway calculated for the reaction between HZnNH_2 with CO_2 leading to the carbamate $\text{HZnO}_2\text{CNH}_2$.

The calculations were repeated with the more realistic model compound methylzinc dimethylamide, $\text{H}_3\text{CZnN}(\text{CH}_3)_2$. For this molecule the effect of changing the method from the pure DFT method BP to the hybrid method B3LYP, which generally gives more accurate energies, was also analyzed. The energy curves resulting from these calculations are included in Figure 2. It can be seen that the reaction mechanism is qualitatively and in some important details also quantitatively similar to that obtained for HZnNH_2 . Again, a ΔG barrier of ca. $60 \text{ kJ}\cdot\text{mol}^{-1}$ leads from the separated reactants to the intermediate, which is, however, this time more strongly bound ($\Delta E = -40 \text{ kJ}\cdot\text{mol}^{-1}$, instead of $-19 \text{ kJ}\cdot\text{mol}^{-1}$ in the case of HZnNH_2). A small barrier separates this intermediate from the carbamate product, which is now bound by $\Delta E = -105 \text{ kJ}\cdot\text{mol}^{-1}$ (instead of $-79 \text{ kJ}\cdot\text{mol}^{-1}$ in the case of HZnNH_2). The values calculated for the relative energies with and without zero-point energy corrections, and for the standard Gibbs energy are summarized in Table 1. BP and B3LYP give similar relative energies.

Table 2 summarizes the energy changes calculated for reactions of several different monomeric model alkylzinc amides with CO_2 to give monomeric carbamates. All carbamates prefer structure type **B** (see Scheme 2). Facile oligomerization reactions of the monomeric carbamates should therefore be responsible for the fact that this mode is so seldom realized (see Introduction). On the other hand, the hypothesis that the electron density donated by the two oxy-

gen atoms is so great that the highly strained four-membered ring of **B** generally cannot form^[24] can be ruled out. It can be seen that the reaction energy is very sensitive to variations of the amide group (see Figure 4). Thus the reaction energy increases in the order $\text{NF}_2 < \text{N}(\text{Ph})_2 < \text{N}(\text{H})\text{Ph} < \text{NH}_2 < \text{N}(\text{iPr})_2$, a trend that can easily be explained by the increasing basicity. On the other hand, the reaction energy is not significantly different for HZnNH_2 , CH_3ZnNH_2 , and CF_3ZnNH_2 indicating that the energies are less sensitive to alterations on the alkyl side. Table 3 compares the Zn–N distances in the initial alkylzinc amides and the Zn–O distances in the carbamate products with the reaction energy. In general large Zn–N distances of the alk-

Table 2. Reaction energies (in $\text{kJ}\cdot\text{mol}^{-1}$) as calculated with BP/SVP and BP/TZVPP for reactions starting with monomeric HZnNH_2 .

Reaction	BP/SVP	BP/TZVPP
$\text{HZnNH}_2 + \text{CO}_2 \rightarrow \text{HZnO}_2\text{CNH}_2$	-115	-79
$\text{H}_3\text{CZnNH}_2 + \text{CO}_2 \rightarrow \text{H}_3\text{CZnO}_2\text{CNH}_2$	-114	-78
$\text{H}_3\text{CZnN}(\text{CH}_3)_2 + \text{CO}_2 \rightarrow \text{H}_3\text{CZnO}_2\text{CN}(\text{CH}_3)_2$	-132	-105
$\text{F}_3\text{CZnNH}_2 + \text{CO}_2 \rightarrow \text{F}_3\text{CZnO}_2\text{CNH}_2$	-112	-76
$\text{H}_3\text{CZnNF}_2 + \text{CO}_2 \rightarrow \text{H}_3\text{CZnO}_2\text{CNF}_2$	-43	-8
$\text{HZnN}(\text{iPr})_2 + \text{CO}_2 \rightarrow \text{HZnO}_2\text{CN}(\text{iPr})_2$	-124	-97
$\text{H}_3\text{CZnN}(\text{iPr})_2 + \text{CO}_2 \rightarrow \text{H}_3\text{CZnO}_2\text{CN}(\text{iPr})_2$	-123	-96
$\text{HZnN}(\text{H})\text{Ph} + \text{CO}_2 \rightarrow \text{HZnO}_2\text{CN}(\text{H})\text{Ph}$	-88	-61
$\text{HZnN}(\text{Ph})_2 + \text{CO}_2 \rightarrow \text{HZnO}_2\text{CN}(\text{Ph})_2$	-71	-31
$2 [\text{HZnO}_2\text{CNH}_2] \rightarrow [\text{HZnO}_2\text{CNH}_2]_2$	-116	-76
$2 [\text{HZnO}_2\text{CNH}_2]_2 \rightarrow [\text{HZnO}_2\text{CNH}_2]_4$	-162	-103
$4 [\text{HZnO}_2\text{CNH}_2] \rightarrow [\text{HZnO}_2\text{CNH}_2]_4$	-393	-255
$\text{H}_3\text{CZnO}_2\text{CN}(\text{iPr})_2 \rightarrow [\text{H}_3\text{CZnO}_2\text{CN}(\text{iPr})_2]_4$	-325	^[a]

[a] Because of computational restrictions the calculation for this special reaction has been performed exclusively with BP/SVP.

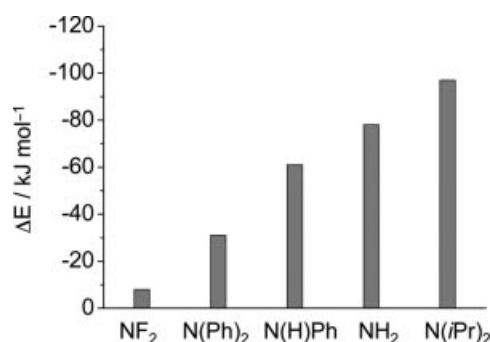


Figure 4. Energy changes for the reactions between CO_2 and Zn amides of the general formula HZnNRR' ($\text{R}, \text{R}' = \text{H}, \text{F}, \text{Ph}, \text{iPr}$).

Table 3. Zn–N distance (in pm) in the reactant and Zn–N distance (also in pm) in the product as well as reaction energies (in $\text{kJ}\cdot\text{mol}^{-1}$) as calculated with BP/TZVPP for some zinc amides.

Reactant	$d(\text{Zn}-\text{N})$, reactant	$d(\text{Zn}-\text{O})$, product	ΔE
HZnNF_2	195.4	210.5	-8
$\text{HZnN}(\text{H})\text{F}$	188.0	205.6/208.1	-56
HZnNPh_2	186.6	204.4	-31
$\text{HZnN}(\text{H})\text{Ph}$	183.8	203.1/207.3	-61
HZnNH_2	183.1	204.6	-78
$\text{HZnN}(\text{iPr})_2$	183.3	203.4	-97

ylzinc amide reactant lead to large Zn–O distances in the carbamate product and consequently smaller values of the absolute reaction energies.

Oligomerization of Monomeric Carbamates

The final step in our model reaction pathway is oligomerization of the monomeric carbamates. Tetramers seem to represent the preferred end products. Figure 5 visualizes the oligomerization process for the simplest model reactant HZnNH_2 leading first to dimers and finally to tetramers. Dimerization of two carbamate monomers is associated with an energy change of -116 (BP/SVP) or -76 $\text{kJ}\cdot\text{mol}^{-1}$ (BP/TZVPP). The zero-point corrected energy change and the ΔG value for this process are -71 and -19 $\text{kJ}\cdot\text{mol}^{-1}$, respectively (BP/TZVPP). The dimer is unsymmetrical (C_1 symmetry) and features C–O, Zn–H, Zn–O, and C–N bond lengths of 127.8–128.7, 153.0, 197.5–199.3, and 136.2 pm, respectively. The O–Zn–O and O–C–O bond angles measure 99.8° and $124.3/125.0^\circ$. Further dimerization of these dimers to give tetramers is even more exothermic [reaction energies of -162 (BP/SVP) or -103 $\text{kJ}\cdot\text{mol}^{-1}$ (BP/TZVPP) and $\Delta G = -36$ $\text{kJ}\cdot\text{mol}^{-1}$ (BP/TZVPP)]. To test the accuracy of our calculations we have also calculated the structure of

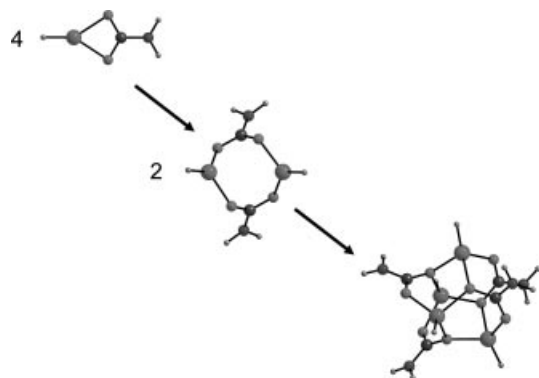


Figure 5. Pathway leading to the $[\text{HZnO}_2\text{CNH}_2]_4$ tetramer starting with a HZnNH_2 monomer.

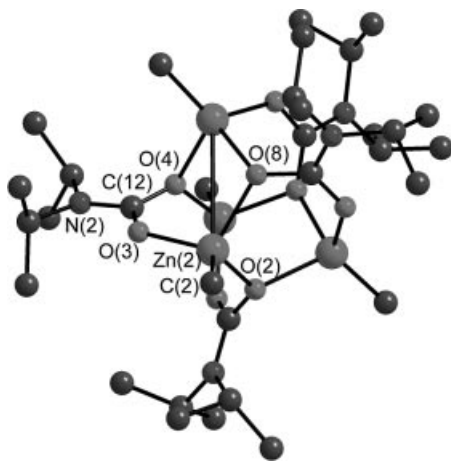


Figure 6. Experimentally determined structure of the $[\text{MeZnO}_2\text{C-N}(\text{iPr})_2]_4$ tetramer (see ref.^[14]). H atoms are omitted for the sake of clarity.

$[\text{H}_3\text{CZnO}_2\text{CN}(\text{iPr})_2]_4$ (only with BP/SVP because of computational restrictions) and compared it to the experimentally observed one. Figure 6 shows the structure of $[\text{CH}_3\text{ZnO}_2\text{CN}(\text{iPr})_2]_4$ from the literature^[17] and Table 4 compares the experimentally obtained dimensions with the corresponding calculated ones for $[\text{MeZnO}_2\text{CN}(\text{iPr})_2]_4$ and $[\text{HZnO}_2\text{CNH}_2]_4$. The labeling of the atoms as shown in Figure 6 and Table 4 is taken from ref.^[17] It can be seen that the general level of agreement between the calculated and experimentally observed dimensions is already good with BP/SVP.

Table 4. Comparison between experimental dimensions (bond lengths in pm, bond angles in $^\circ$) for $[\text{MeZnO}_2\text{CN}(\text{iPr})_2]_4$ (from ref.^[14]) and calculated ones for $[\text{MeZnO}_2\text{CN}(\text{iPr})_2]_4$ and $[\text{HZnO}_2\text{CNH}_2]_4$.

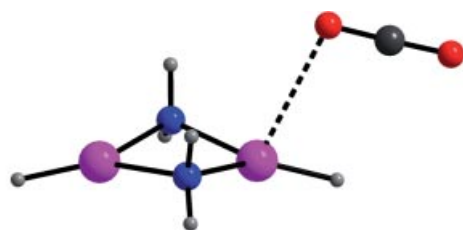
Parameter ^[a]	$[\text{MeZnO}_2\text{CN}(\text{iPr})_2]_4$ exp. ^[b]	$[\text{MeZnO}_2\text{CN}(\text{iPr})_2]_4$ calcd.	$[\text{HZnO}_2\text{CNH}_2]_4$ calcd.
Zn(2)–C(2)	195.0(3)	197.7	–
Zn(2)–O(2)	208.8(2)	210.5	215.7
Zn(2)–O(3)	199.2(2)	201.5	202.0
Zn(2)–O(8)	205.5(2)	210.3	208.7
O(3)–C(12)	125.9(3)	127.4	126.8
C(12)–O(4)	130.8(3)	131.3	130.4
C(12)–N(2)	133.9(3)	136.7	135.5
O(3)–Zn(2)–O(8)	101.98(7)	100.0	99.2
O(2)–Zn(2)–O(3)	100.54(7)	98.4	96.9
O(2)–Zn(2)–O(8)	93.45(6)	92.9	91.8
O(3)–C(12)–O(4)	121.0(2)	122.3	124.7

[a] See Figure 6 for atom numbering. [b] Ref.^[14]

2. Reactions Starting from Dimeric Alkylzinc Amides

There are numerous examples of authenticated dimeric alkylzinc amides. However, their structural analysis using X-ray diffraction is limited. Just to name two of them, the crystal structures of dimeric methylzinc and ethylzinc triisopropylsilylamide have recently been reported.^[25] Dimerization of the model compound HZnNH_2 to give cyclic $[\text{HZnNH}_2]_2$ is associated with an energy change of -189 $\text{kJ}\cdot\text{mol}^{-1}$ according to BP/SVP and -133 $\text{kJ}\cdot\text{mol}^{-1}$ according to BP/TZVPP calculations. In addition to DFT calculations using the BP functional ab initio (MP2) calculations were performed in this special case to test the accuracy of our calculated methods. MP2/TZVPP calculations gave a dimerization energy of -157 $\text{kJ}\cdot\text{mol}^{-1}$. Thus the energies calculated with DFT methods are relatively close to those calculated with MP2. The standard Gibbs energy change for dimerization, ΔG° , was calculated to be -75 $\text{kJ}\cdot\text{mol}^{-1}$ according to BP/TZVPP and -99 $\text{kJ}\cdot\text{mol}^{-1}$ according to MP2/TZVPP. The Zn–H, Zn–N, and N–H distances in the dimer amount to 154.6, 204.6, and 102.3 pm, respectively, and the N–Zn–N and Zn–N–Zn bond angles were calculated to be 86.9° and 93.1° , respectively. In the case of $[\text{MeZnN}(\text{iPr})_2]_2$, an example for which crystal structures are available,^[28] the Zn–N distances, and N–Zn–N and Zn–N–Zn bond angles were experimentally determined to be 201.5–204.0 pm, 89.8 – 90.0° , and 90.1 – 90.2° , respec-

tively. Thus the experimental values are in good agreement with the ones calculated for the model dimer $[\text{HZnNH}_2]_2$.



Structure of the complex $[(\text{HZnNH}_2)_2(\text{CO}_2)]$

CO_2 first forms only a weakly bound complex with $[\text{HZnNH}_2]_2$. The binding energy amounts to no more than $-11 \text{ kJ}\cdot\text{mol}^{-1}$ according to BP/SVP and $-5 \text{ kJ}\cdot\text{mol}^{-1}$ according to BP/TZVPP. In this complex, the Zn atom interacts with one of the O atoms of CO_2 , the distance being ca. 298 pm. The N and C atoms are separated by ca. 460 pm. As anticipated, the dimer does not allow any attractive $\text{N}\cdots\text{C}$ interaction to be established (all valence orbitals on the N atoms are engaged in bonding with the H and Zn atoms of the $[\text{HZnNH}_2]_2$ unit). A vibrational analysis (at the BP/SVP level) confirmed that this complex defines a minimum on the potential energy surface.

Part a of Figure 7 displays the relative energy versus the separation between the carbon atom of the CO_2 molecule and one of the N atoms. It can be seen that the energy first increases (extremely sharply between 240 and 232 pm) until a transition state is reached at 232.8 pm. The sharp increase coincides with a large increase in the Zn–N bond length into which CO_2 first inserts (from 208.9 pm at an $\text{N}\cdots\text{C}$ distance of 238.1 pm to 285.5 pm for an $\text{N}\cdots\text{C}$ distance of 232.8 pm). The transition state energy is $51 \text{ kJ}\cdot\text{mol}^{-1}$ higher than the sum of the energies of the separated reactants. ΔG at this point amounts to $+103 \text{ kJ}\cdot\text{mol}^{-1}$ (see Table 5). The barrier is caused by the weakening of the strong Zn–N bonds, which cannot be compensated by the newly formed C–N and O–Zn interactions. The transition state is further characterized by Zn \cdots O and N \cdots C distances of 228.9 and 232.9 pm, respectively. The C–O distances measure 120.1 and 117.6 pm. Thus one of the C–O distances is already significantly elongated with respect to the distance in free CO_2 (117.1 pm). We therefore conclude that the reaction of the dimeric alkylzinc amide is subjected to a significantly higher barrier than that starting from the monomer. It is also higher than that calculated for the reaction between dimeric lithium amides and CO_2 (a Gibbs free energy barrier of $+41 \text{ kJ}\cdot\text{mol}^{-1}$ was obtained in this work).^[14] In the case of the lithium amides, the Li–N distance seems to be insignificantly elongated at the transition state.

For smaller distances the energy decreases again, but not steadily, until the carbamate is formed. A local minimum is reached at 148.6 pm exhibiting a relative energy of $-19 \text{ kJ}\cdot\text{mol}^{-1}$ ($\Delta G = +33 \text{ kJ}\cdot\text{mol}^{-1}$) and featuring a six-membered $[\text{ZnNZnNCO}]$ ring. A vibrational analysis confirms that it is a real minimum (no imaginary frequencies occurred). The Zn–N–C angle at this point amounts to 105.9° . If we introduce the atom numbers N1, N2, Zn1,

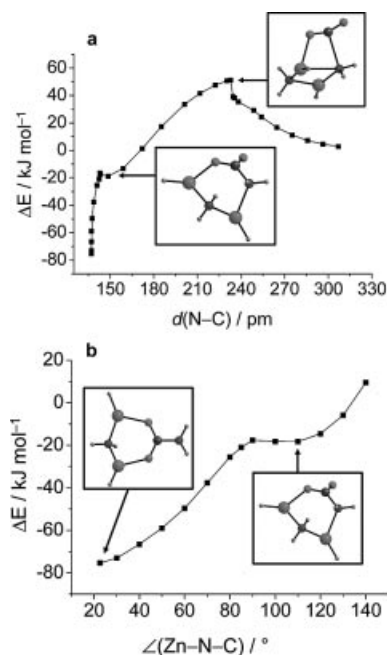


Figure 7. (a) Energy versus the N–C separation and relative to the separated reactants for the reaction of the $[\text{HZnNH}_2]_2$ dimer with CO_2 . (b) Energy versus the Zn–N–C angle and relative to the separated reactants for the reaction of the $[\text{HZnNH}_2]_2$ dimer with CO_2 .

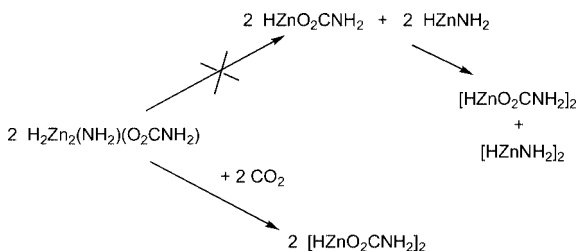
Table 5. Energy, ΔE , zero-point energy corrected energy, ΔE_{ZPE} , and ΔG (at 298 K, 1 bar), all in $\text{kJ}\cdot\text{mol}^{-1}$, relative to the reactants for the reaction between $[\text{HZnNH}_2]_2$ and CO_2 as calculated with BP/TZVPP.

	ΔE	ΔE_{ZPE}	ΔG
First TS ^[a]	+51	+65	+103
Intermediate	-19	-5	+34
Second TS ^[a]	-18	-4	+35
Product	-75	-63	-24

[a] TS: transition state.

Zn2, O1, and O2, with Zn1 being bound to O1 and N1, and Zn2 being bound to N1 and N2, the bond lengths (in pm) are as follows: 203.7 (Zn1–N1), 197.2 (Zn2–N1), 218.2 (Zn2–N2), 148.6 (N2–C), 129.0 (C–O1), 122.3 (C–O2), 198.2 (O1–Zn1). The Zn1 \cdots N2 separation amounts to 351.7 pm. The changes in the C–N distance between the structure of this local minimum (148.6 pm) and the carbamate product (136.9 pm) are relatively small. In fact toward the end of the reaction the C–N distance remains almost unchanged although the energy still decreases. Therefore for this stage of the reaction, the C–N distance is not the optimal choice for the reaction coordinate and the Zn–N–C bond angle was taken instead. The corresponding energy curve is displayed in Figure 7b. It can be seen that the barrier separating the intermediate from the heterodimer $[\text{H}_2\text{Zn}(\text{NH}_2)(\text{O}_2\text{CNH}_2)]$ amounts to no more than $1.3 \text{ kJ}\cdot\text{mol}^{-1}$. The overall reaction to give the heterodimer product is associated with an energy change of $-102 \text{ kJ}\cdot\text{mol}^{-1}$ according to BP/SVP and $-75 \text{ kJ}\cdot\text{mol}^{-1}$ according to BP/TZVPP. ΔG for the overall reaction is $-24 \text{ kJ}\cdot\text{mol}^{-1}$ (BP/TZVPP). The nonplanar product is char-

acterized by the following distances (in pm) and angles: 128.1 (C–O), 200.2 (Zn–O), 200.0 (Zn–N), 136.9 (C–N), 127.2° (O–C–O), and 106.5° (Zn–N–Zn). In summary, the rate-determining step again turns out to be the formation of the intermediate, which is opposed by a barrier ΔG of +103 kJ·mol^{−1}.



Further Reaction with CO₂ and Oligomerization

Two possible routes lead from the heterodimer $\text{H}_2\text{Zn}_2(\text{O}_2\text{CNH}_2)(\text{NH}_2)$ to the homodimer $[\text{HZnO}_2\text{CNH}_2]_2$. The first one includes dissociation of $\text{H}_2\text{Zn}_2(\text{O}_2\text{CNH}_2)(\text{NH}_2)$ to give monomeric $\text{HZnO}_2\text{CNH}_2$ and HZnNH_2 , which afterwards dimerize to $[\text{HZnO}_2\text{CNH}_2]_2$ and $[\text{ZnNH}_2]_2$, respectively. The energy needed to form the monomers is, however, 176 (BP/SVP) or 129 kJ·mol^{−1} (BP/TZVPP). The subsequent dimerization is, of course, exothermic, but the overall formation of $[\text{HZnO}_2\text{CNH}_2]_2$ and $[\text{ZnNH}_2]_2$ is still endothermic (see Table 6). The second possibility is that $[\text{HZnO}_2\text{CNH}_2]_2$ is formed by the reaction between $\text{H}_2\text{Zn}_2(\text{O}_2\text{CNH}_2)(\text{NH}_2)$ and a second CO₂ molecule. This reaction is calculated to be exothermic [reaction energy of −55 (BP/SVP) or −26 kJ·mol^{−1} (BP/TZVPP)], and therefore this most likely represents the preferred path. It is worth mentioning that our calculations show that the fixation of the first CO₂ molecule (reaction energy of −75 kJ·mol^{−1} according to BP/TZVPP) is significantly more exothermic than the fixation of the second one (reaction energy of only −26 kJ·mol^{−1}). While ΔG for the fixation of the first CO₂ is negative (−24 kJ·mol^{−1}), it is positive (+34 kJ·mol^{−1}) for the fixation of the second one. It has been shown that in enzymes the presence of a carbamate ligand is important for CO₂ fixation. Carbamate formation preorganizes the active center e.g. of the Mg²⁺ complex in the center of the enzyme rubisco. The carbamate ligand adopts in this special case an end-on monodentate rather than a bidentate coordination mode,

which is different from our model compounds. Figure 8 shows the reaction pathway leading first to $[\text{H}_2\text{Zn}_2(\text{NH}_2)(\text{O}_2\text{CNH}_2)]$ and then to $[\text{HZnO}_2\text{CNH}_2]_2$. This molecule dimerizes finally to the tetramer as shown in Figure 5. This dimerization is accompanied by an energy change of −103 kJ·mol^{−1}. ΔG for this process is −36 kJ·mol^{−1}.

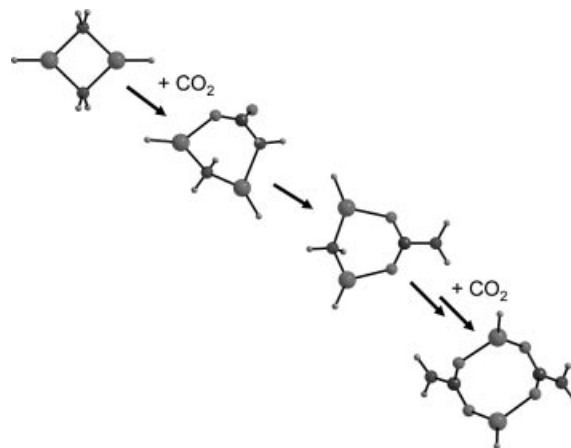


Figure 8. Pathway from $[\text{HZnNH}_2]_2$ and CO₂ leading to the $[\text{HZnO}_2\text{CNH}_2]_2$ homodimer that later dimerizes as shown in Figure 5.

Conclusions

Quantum chemical calculations were used to obtain detailed insight into CO₂ fixation by monomeric as well as dimeric alkylzinc amides. The reaction of monomeric alkylzinc amides first leads to an intermediate featuring a four-membered $[\text{ZnNCO}]$ ring. The activation energy ΔG of this first, rate-determining step is around +60 kJ·mol^{−1}. From this local minimum on the potential energy surface the system has to pass a much smaller barrier to proceed to the monomeric carbamate product. Dimerization and tetramerization of the monomeric carbamates follow (both exhibiting negative ΔG values). Any engagement of an N-bonded carbamate species during the reaction can be ruled out. CO₂ fixation by several different alkylzinc amide molecules bearing the overall formula $\text{RZnNR}'\text{R}''$ was then compared. The reaction energies were found to be highly sensitive to changes in the electronic properties of the amido group, while modifications on the alkyl (R) side bear almost no influence.

The calculations indicate that the reaction of dimeric alkylzinc amides with CO₂ is opposed by a larger barrier (ΔG value more than +100 kJ·mol^{−1}). In this case the transition state features a four-membered $[\text{ZnNCO}]$ ring. A six-membered ring then follows as a local minimum on the potential energy curve. The barrier separating this intermediate from the product is again very small. Surprisingly, the calculations indicate that the barrier for CO₂ fixation by dimeric alkylzinc amides is higher than the negative dimerization energy of the monomeric alkylzinc amide. It is also higher than the barrier for CO₂ fixation by monomeric alkylzinc

Table 6. Reaction energies (in kJ·mol^{−1}) as calculated with BP/SVP and BP/TZVPP for reactions involving the $[\text{HZnNH}_2]_2$ dimer.

Reaction	BP/SVP	BP/TZVPP
$2 \text{ HZnNH}_2 \rightarrow [\text{HZn}(\mu\text{-NH}_2)]_2$	−189	−133
$[\text{HZn}(\mu\text{-NH}_2)]_2 + \text{CO}_2 \rightarrow \text{H}_2\text{Zn}_2(\text{O}_2\text{CNH}_2)(\text{NH}_2)$	−102	−75
$\text{H}_2\text{Zn}_2(\text{O}_2\text{CNH}_2)(\text{NH}_2) + \text{CO}_2 \rightarrow [\text{HZn}(\text{O}_2\text{CNH}_2)]_2$	−55	−26
$\text{H}_2\text{Zn}_2(\text{O}_2\text{CNH}_2)(\text{NH}_2) \rightarrow \text{HZn}(\text{O}_2\text{CNH}_2) + \text{HZnNH}_2$	+176	+129
$[\text{HZn}(\text{O}_2\text{CNH}_2)]_2 \rightarrow 2 \text{ HZn}(\text{O}_2\text{CNH}_2)$	+116	+76
$2 \text{ H}_2\text{Zn}_2(\text{O}_2\text{CNH}_2)(\text{NH}_2) \rightarrow [\text{HZn}(\text{O}_2\text{CNH}_2)]_2 + [\text{HZnNH}_2]_2$	+48	+49

amide (ca. 60 kJ·mol⁻¹). Therefore, although dimeric alkylzinc amides are preferred over monomers, reaction with CO₂ could very well predominantly occur from the monomeric state.

Computational Details

Calculations were carried out with the aid of the TURBOMOLE program package.^[26] Pure DFT calculations relied on the BP method (BP is the short notation for Becke–Perdew and is a nonlocal DFT method employing the Becke exchange and Perdew correlation functionals). In addition the hybrid-method B3LYP (DFT using Becke exchange functional and Lee–Yang–Parr correlation functional, as well as Hartree–Fock exchange)^[27] was used in the mechanistic studies since this method generally leads to more accurate energies.

It has been shown in the case of quantum chemical studies on CO₂ fixation by lithium amides^[14] that the choice of basis set is important and that large basis sets (ideally including polarization functions) are necessary. Therefore for all our calculations we have used not only an SVP (split-valence, polarized), but also a TZVPP (triple-zeta valence, doubly-polarized) basis set.^[28] It turned out that the reaction energies as calculated with the SVP basis set are in some cases different from those calculated with the TZVPP basis set.

It should be mentioned that for the mechanistic studies it is assumed, as in almost all mechanistic studies of this kind, that the reaction can be divided into several steps, e.g. the dimeric alkylzinc amide reacts in the first step with one equivalent of CO₂ and afterwards in a second step with another equivalent of CO₂. Of course it is plausible that the reaction with a second CO₂ already occurs before completion of the reaction with the first one, and this should indeed happen if it leads to lower energies. However, it is almost impossible to consider all reaction pathways. The “step-by-step” hypothesis thus leads to an upper limit for the true reaction barrier.

In the mechanistic studies a vibrational analysis was carried out at each point to make sure that the approach of the two reactants occurs along a low-energy path. The relative energies, zero-point corrected energies, and the Gibbs energies of all the important points along the reaction path are included in the discussion (see also Tables 1 and 5). Solvent effects were not considered. The solvent used in most of the synthetic work is toluene. The interaction between toluene and the two reactants is expected to be small. In addition, the accurate description of interactions of this kind, which involve the π system of toluene, is extremely difficult and requires highly sophisticated and practically unusable methods to model the complete reaction mechanism.

Acknowledgments

Financial support from the Deutsche Forschungsgemeinschaft (DFG) and the Fonds der Chemischen Industrie is gratefully acknowledged.

- [1] See, for example: P. B. Reich, S. E. Hobbie, T. Lee, D. S. Ellsworth, J. B. West, D. Tilman, J. M. H. Knops, S. Naeem, J. Trost, *Nature* **2006**, *440*, 922; and references therein.
- [2] See, for example: a) K. K. Pandey, *Coord. Chem. Rev.* **1995**, *140*, 37–114; b) W. Leitner, *Coord. Chem. Rev.* **1996**, *153*, 257.
- [3] I. Castro-Rodriguez, H. Nakai, L. N. Zakharov, A. L. Rheingold, K. Meyer, *Science* **2004**, *305*, 1757.

- [4] C.-C. Chang, M.-C. Liao, T.-H. Chang, S.-M. Peng, G.-H. Lee, *Angew. Chem.* **2005**, *117*, 7584; *Angew. Chem. Int. Ed.* **2005**, *44*, 7418.
- [5] H. Phull, D. Alberti, I. Korabkov, S. Gambarotta, P. H. M. Budzelaar, *Angew. Chem.* **2006**, *118*, 5457.
- [6] See, for example: a) M. Ruf, H. Vahrenkamp, *Inorg. Chem.* **1996**, *35*, 6571; b) M. Ruf, F. A. Schell, R. Walz, H. Vahrenkamp, *Chem. Ber./Recueil* **1997**, *130*, 101; c) H. Vahrenkamp, *Acc. Chem. Res.* **1999**, *32*, 589; d) A. Peter, H. Vahrenkamp, *Z. Anorg. Allg. Chem.* **2005**, *631*, 2347, and references therein.
- [7] See, for example: B. Bauer-Siebenlist, F. Meyer, E. Farkas, D. Vidovic, S. Dechert, *Chem. Eur. J.* **2005**, *11*, 4349.
- [8] C.-C. Chang, M. S. Ameerunisha, *Coord. Chem. Rev.* **1999**, *189*, 199.
- [9] a) T. C. Taylor, I. Andersson, *Nat. Struct. Biol.* **1996**, *3*, 95; b) J. Newman, S. Gutteridge, *Structure* **1994**, *2*, 495; c) W. W. Cleland, T. J. Andrews, S. Gutteridge, F. C. Hartman, G. H. Lorimer, *Chem. Rev.* **1998**, *98*, 549, and references therein.
- [10] D. Walther, M. Ruben, S. Rau, *Coord. Chem. Rev.* **1999**, *182*, 67; and references therein.
- [11] a) E. Jabry, M. B. Car, P. Hausinger, P. A. Karplus, *Science* **1995**, *268*, 998; b) L. S. Park, R. P. Hausinger, *Science* **1995**, *267*, 1156.
- [12] Y. Tang, L. N. Zakharov, A. L. Rheingold, R. A. Kemp, *Organometallics* **2004**, *23*, 4788.
- [13] U. Köhn, E. Anders, *Tetrahedron Lett.* **2002**, *43*, 9585.
- [14] S. O. N. Lill, U. Köhn, E. Anders, *Eur. J. Org. Chem.* **2004**, 2868.
- [15] M. B. Hursthouse, M. A. Malik, M. Motevalli, P. O'Brien, *J. Chem. Soc., Chem. Commun.* **1991**, 1690.
- [16] I. Abrahams, M. A. Malik, M. Motevalli, P. O'Brien, *J. Chem. Soc., Dalton Trans.* **1995**, 1043.
- [17] Y. Tang, W. S. Kassel, L. N. Zakharov, A. L. Rheingold, R. A. Kemp, *Inorg. Chem.* **2005**, *44*, 359.
- [18] M. Westerhausen, M. Wieneke, W. Schwarz, *J. Organomet. Chem.* **1999**, *572*, 249.
- [19] Variable-temperature NMR spectroscopic studies have shown that the dimeric structure of the amide $\{[(\text{PhCH}_2)_2\text{N}]_2\text{Zn}\}_2$ fails to remain wholly intact in arene solution and a dynamic monomer–dimer equilibrium exists. See: D. R. Armstrong, G. C. Forbes, R. E. Mulvey, W. Clegg, D. M. Tooke, *J. Chem. Soc., Dalton Trans.* **2002**, 1656.
- [20] D. J. Darensbourg, W.-Z. Lee, A. L. Phelps, E. Guidry, *Organometallics* **2003**, *22*, 5585.
- [21] S. Park, A. L. Rheingold, D. M. Roundhill, *Organometallics* **1991**, *10*, 615.
- [22] The start and end geometries exhibit both C_{2v} symmetry, but the mirror plane changes.
- [23] Calculations were also carried out for CO₂ fixation by the analogue magnesium model compound HMgNH₂ to obtain information on the effect that variation of the metal atom brings about. This reaction was shown to follow the same pattern as that of the Zn compound. The “vertical” approach again leads to a small minimum, which this time adopts a Mg–N–C angle of 109.8° and an energy relative to the sum of the energies of the separated reactants of –25 (BP/SVP) or –6 kJ·mol⁻¹ (BP/TZVPP). The interatomic distances (Mg–N 191.6, C–O 117.3, C···N 302.3 pm) and the O–C–O angle (176.1°) again indicate that the geometries of the two reactants are only slightly influenced by this adduct formation. The intermediate featuring a four-membered Mg–N–C–O ring formed in the course of the “parallel” approach now exhibits a relative energy of –127 (BP/SVP) or –79 kJ·mol⁻¹ (BP/TZVPP). It is reached at a Zn–N–C angle of 84.5°. The Mg–N, N–C, and C–O distances are 215.2, 157.4, and 128.8/120.9 pm, respectively, and the O–C–O bond angle measures 132.9°. With –198 (BP/SVP) or –153 kJ·mol⁻¹ (BP/TZVPP) the overall reaction energy for carbamate formation is almost twice as large as that for the Zn compound.
- [24] K.-C. Yang, C.-C. Chang, C.-S. Yeh, G.-H. Lee, S.-M. Peng, *Organometallics* **2001**, *20*, 126.

- [25] M. Westerhausen, T. Bollwein, A. Pfitzner, T. Nilges, H.-J. Deiseroth, *Inorg. Chim. Acta* **2001**, 312, 239.
- [26] a) R. Ahlrichs, M. Bär, M. Häser, H. Horn, C. Kölmel, *Chem. Phys. Lett.* **1989**, 162, 165; b) K. Eichkorn, O. Treutler, H. Öhm, M. Häser, R. Ahlrichs, *Chem. Phys. Lett.* **1995**, 240, 283; c) K. Eichkorn, O. Treutler, H. Öhm, M. Häser, R. Ahlrichs, *Chem. Phys. Lett.* **1995**, 242, 652; d) K. Eichkorn, F. Weigend, O. Treutler, R. Ahlrichs, *Theor. Chem. Acc.* **1997**, 97, 119; e) F. Weigend, M. Häser, *Theor. Chem. Acc.* **1997**, 97, 331; f) F. Weigend, M. Häser, H. Patzelt, R. Ahlrichs, *Chem. Phys. Lett.* **1998**, 294, 143.
- [27] a) A. D. Becke, *J. Chem. Phys.* **1993**, 98, 5648; b) P. J. Stephens, F. J. Devlin, C. F. Chabalowski, M. J. Frisch, *J. Phys. Chem.* **1994**, 98, 11623.
- [28] A. Schäfer, H. Horn, R. Ahlrichs, *J. Chem. Phys.* **1992**, 97, 2571.

Received: September 8, 2006

Published Online: January 4, 2007